

## Study on the influence of output inductance on DBD plasma uniformity

MARCIN HOŁUB

*Faculty of Electrical Engineering, West Pomeranian University of Technology  
Sikorskiego 37, 70-313 Szczecin, Poland  
tel.: +48 91 449 4805., fax: +48 91 449 4317  
e-mail: marcin.holub@zut.edu.pl  
URL: <http://www.we.zut.edu.pl>*

(Received: 11.02.2014, revised: 27.03.2014)

**Abstract:** The presented work gives an overview on simulation and experimental results of the power supply parameters' influence on DBD discharge uniformity. The proposed study is about the use of quasi-pulsed, power electronic power supply and a saturable inductor in series with the discharge cell [1]. The simulation results are presented with a parallel DBD reactor model with linear critical voltage distribution. A more uniform current waveform is observed, however, due to small reactor capacitances no streamer formation could be verified in calculations. An experimental test stand was prepared with a double dielectric barrier discharge arrangement. The experimental results are presented with regard to the electrical oscilloscope waveforms and ICCD camera imaging. A more homogenous plasma was observed in the case of saturable inductor with saturation current set at the point of discharge formation. Two possible mechanisms are connected with this phenomenon – inductive element current support during discharge and/or current rise-time limitation [1].

**Key words:** Non-thermal plasma, power electronic supply, plasma uniformity, dielectric barrier discharge reactors.

### 1. Introduction

The modern applications of plasmas in life sciences or environmental applications require the operation in the non-thermal regime at atmospheric pressure in ambient air or in polluted gas mixture. The dielectric barrier discharges (DBD), coronas and plasma jets respond to these requirements but such plasmas usually show a filamentary character. The high collision rates lead to rapid formation of local space charges and thus the electrical breakdown proceeds in several individual ionization channels, investigated as microdischarges, filaments or plasma bullet trains. However, barrier discharges can be operated in the so-called diffuse modes where the plasma covers the entire electrode area uniformly. Different diffuse modes can be investigated, such as the so-called Atmospheric Pressure Townsend Discharge [2], the Atmospheric Pressure Glow Discharge [3] or the pseudoglow discharge [4].

The presence of uniform plasmas is observed only at selected conditions which include the gas chemical composition and purity, the discharge configuration [5], the frequency of the applied voltage [6] as well as the properties of the external electrical circuit and the power supply [1]. This contribution gives an additional insight into the experimental results obtained with a one-module dielectric barrier discharge (DBD) reactor with variable supply system parameters.

## 2. Power electronic supply unit

The power supply is the integral part of plasma system design influencing not only the chemical reactions but also the overall energy transfer ratio. In many cases classical 50 or 60 Hz supplies are used with high-voltage transformers [7, 8]. Many different voltage waveforms are used for plasma system supply [9, 10].

Due to the operating conditions and necessary power transfer, the higher operation frequency is often necessary and the average power control is also critical for the chemical process intensity. The modern supply system designs include power amplifiers with high-voltage transformers [11, 12] or many solid-state switch-based converter topologies, often resonant ones [13]. The resonant operation makes the fluent control of the output power more complicating, often a time-averaged burst (called the pulse density modulation – PDM) technique is used [14]. The high frequency supplies usually use a rectifier as the first power electronic converter. Then, the different configurations and topologies are used, in many cases a high frequency – high voltage transformer (HF, HV) is used. Sometimes, the additional pulse forming networks are implemented in order to shape the output voltage waveform.

The proposed study featured the use of a quasi-pulsed power supply [15] with variable supply system – reactor coupling inductors. The experimental converter topology is given in Figure 1.

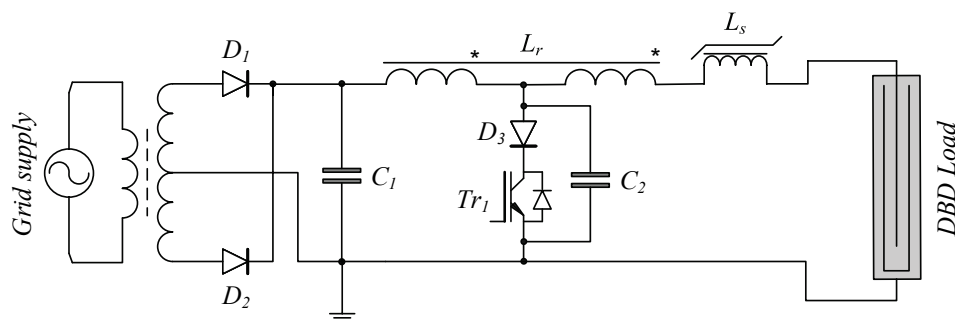


Fig. 1. Topology of a pulsed power electronic converter used for experiments

The converter (Fig. 1) is a coupled inductor  $L_r$ , single transistor topology, with very simple construction, output pulse amplitude can be easily controlled by switch duty factor and the output frequency is easily adjustable. The operation is very similar with flyback switched

mode power supplies but no rectifying diode is used on output. Diode  $D_3$  together with capacitor  $C_2$  form a snubber circuit for the main switch  $Tr_1$  and support the energy balance during the discharge. An additional series inductance  $L_s$  was used in order to investigate the role of nonlinear magnetic behavior on discharge development and uniformity. The main drawbacks of used converter construction include the lack of galvanic separation from the reactor negative electrode as well as unipolar output pulse polarity.

### 3. Simulation model

In order to evaluate the importance of output series inductance a simulation model was prepared in Simplorer 9.0. The power electronic construction was modelled according to the topology presented in Figure 1. An ideal power switch was used as the reactor behavior was examined rather than the power electronic part operation. The constructed model is presented in Figure 2, main simulation parameters are listed in Table 1. The coupled inductor  $L_r$  is simulated using coupled inductors listed as TFR1P1\_1 – TFR1P2\_1 in the schematic.  $C_1$  capacitor was neglected since the ideal voltage source was used for calculations.

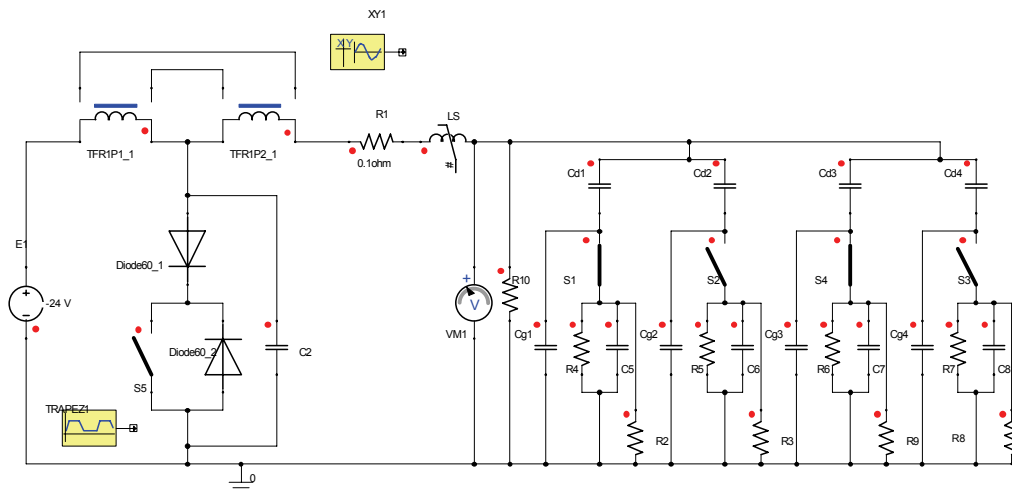


Fig. 2. Simulation model of pulsed power supply and a DBD reactor model

Regarding the DBD reactor modelling a parallel model was used. The equivalent circuit of a DBD reactor was set according to Figure 3, where the reactor is modelled as a series connection of dielectric and gas gap capacitances ( $C_d$  and  $C_g$ ), and in the moment of discharge the gas gap capacitance is shortened by the existing discharge channel with its characteristic resistance  $R_g$ , in parallel to that fact the memory effect capacitor  $C_m$  is charged (simulating partial charge transfer to dielectric surface). This memory effect capacitor is constantly discharged by  $R_m$ . Resistance  $R_o$  simulates overall damping of the discharge unit. The filamentary discharges take place in different parts of the electrode surface and that is why a modular unit with statistically distributed critical voltages of the channel switches is proposed for modeling.

In case of this study 4 such modules were used for simulations ( $n = 4$ ) and a linear critical voltage distribution was used with a minimal, normalized critical voltage of 0.9 p.u. and maximal of 1.1 p.u.

Table 1. Simulation model parameters

Parameter and symbol	Value
Supply voltage E1	24 V
Coupled inductor primary magnetizing inductance TFR1P1_1 $L\mu$	209 $\mu$ H
Coupled inductor primary leakage inductance TFR1P1_1 $Ls$	14 $\mu$ H
Coupled inductor secondary leakage inductance TFR1P1_2 $Ls$	2.8 mH
Overall reactor gas gap capacitance $C_g$	12 pF
Overall reactor dielectric capacitance $C_d$	96 pF
Gas discharge channel resistance R2, R3, R8, R9	10 $\Omega$
Memory effect capacitance C5, C6, C7, C8	0.5 pF
Memory effect resistance R4, R5, R6, R7	1 k $\Omega$
Overall damping resistance R10	1 M $\Omega$

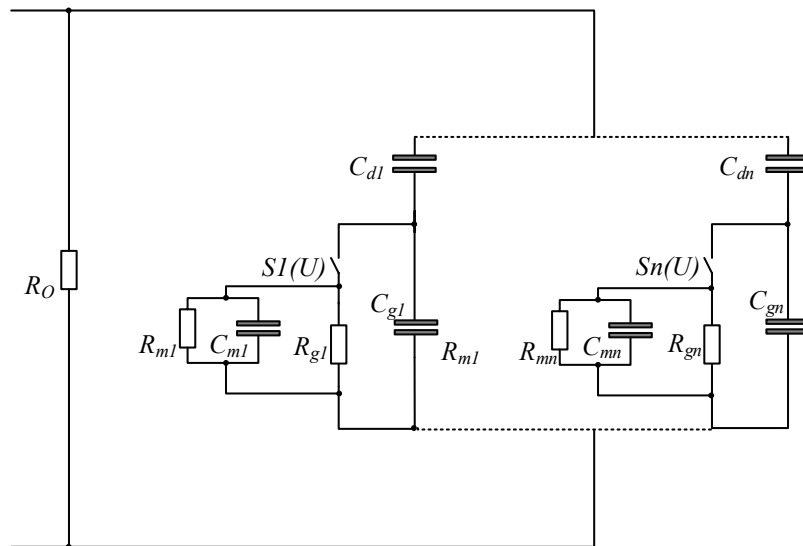


Fig. 3. DBD reactor model

Without additional inductance on the output of the converter only stray inductance of high voltage wires was simulated ( $L_S = 10 \mu$ H in Fig. 2). In such case the overall current delivered by the power supply is:

$$i_s \frac{u_s}{R_O} + i_g, \quad (1)$$

where  $i_s$  is the current delivered by the power supply unit,  $u_s$  is the supply system output voltage,  $i_R$  is the overall reactor current. Prior discharge reactor current can be described as:

$$i_R = C_R \frac{du_S}{dt} \quad (2)$$

and the overall reactor capacitance  $C_R$  is:

$$C_R = \frac{C_d C_g}{C_d + C_g}. \quad (3)$$

After the discharge is initiated:

$$C_d \frac{du_d}{dt} - C_m \frac{du_g}{dt} = u_g \left( \frac{R_m + R_g}{R_m R_g} \right), \quad (4)$$

$$u_d = \frac{1}{C_d} \int i_R(t) dt, \quad (5)$$

$$u_g = u_s - u_d. \quad (6)$$

With nonlinear inductor in series with the power supply only numerical solution can be implemented. Figure 4 gives an example of simulation results for cases with no additional inductance (a) and nonlinear inductor (b) with  $L_s = 37$  mH prior saturation and  $L_s' = 8.4$  mH after saturation. Saturation current was set to  $i_{sat} = 50$  mA. L1.I represents saturable reactor current, Cg1.V and Cd1.V gap and dielectric voltage waveforms, respectively and VM1.V is the overall reactor voltage after the inductor as measured by voltmeter VM1 in Figure 2.

As it can be noticed, the reactor current has much less turbulent character and current rise time was decreased, which can have a positive impact on the discharge uniformity [1]. The short-term streamer discharges are not observed as reactor capacitances and resistances establish time constants in picosecond order of magnitude. The variable capacitance during discharge affects the voltage waveform. The positive impact on the current uniformity during discharge can be expected.

#### 4. Experimental setup and results

In order to examine the supply system influence on discharge uniformity a laboratory DBD discharge cell for atmospheric pressure examinations was constructed. The discharge cell construction is depicted schematically in Figure 5 a, b, below. It consists of brass electrodes with phlogopite plates as a dielectric ( $\epsilon_r \cong 8$ ) with 1 mm gap between dielectrics. The overall discharge area is 95 mm<sup>2</sup>.

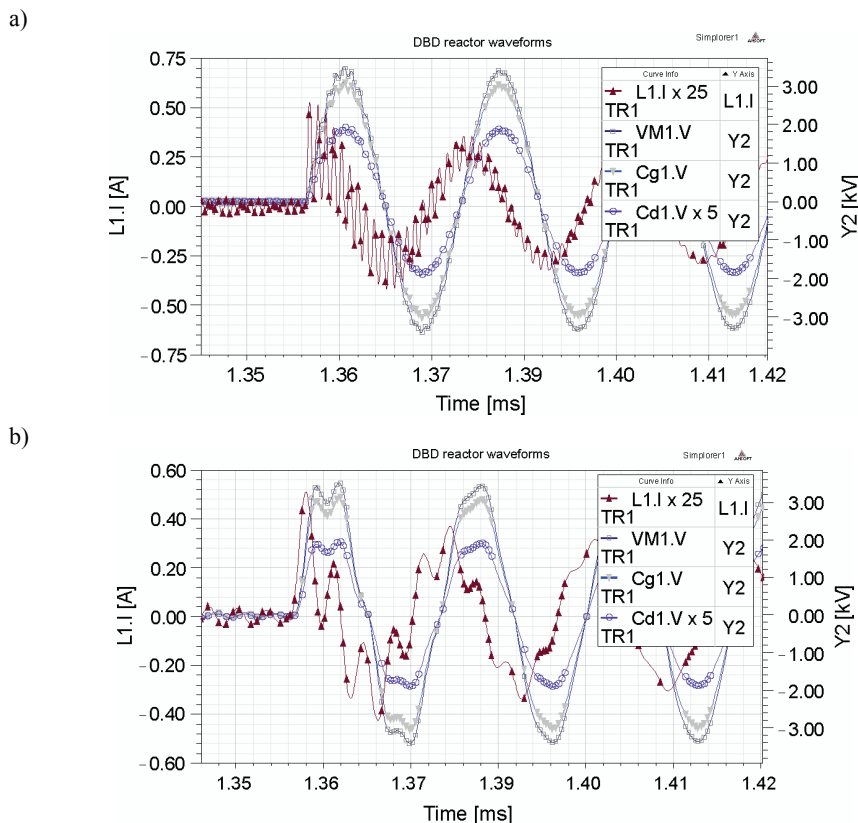


Fig. 4. Converter – reactor waveforms: a) basic configuration without series inductance; b) with series, saturable inductor

The discharge cell body is constructed with the use of Teflon. The plastic bolts were placed for mechanical positioning and fastening. The ambient pressure experiments were conducted in the air, with no forced airflow.

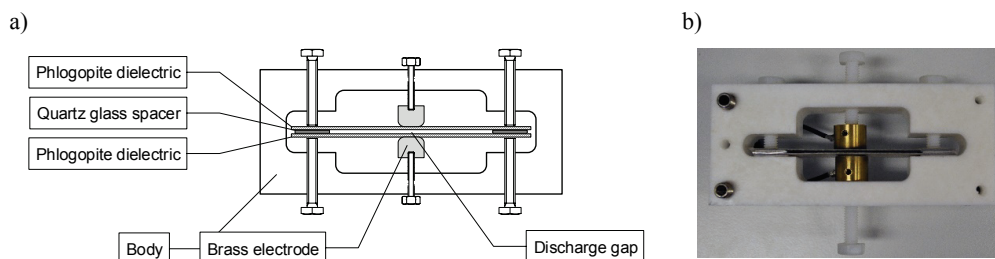


Fig. 5. DBD discharge cell used for examinations: a) basic configuration; b) constructed discharge cell

Different power supply configurations were examined regarding the value and type of serial, nonlinear inductor  $L_s$ . Saturable inductor was prepared with parameters equal to those

used for simulations, CMD5005, toroid material was used. Pulsed waveforms were implemented with 4.6 kHz repetition rate. Plasma uniformity was measured using iCCD (PI-MAXII) imaging with 173  $\mu\text{s}$  exposition time (shutter mode, KAI 1024 $\times$ 1024 detector) and maximal gain of 255. Thus, the results of 1 electric period were observed. The experiments were conducted under ambient pressure in the air. The supply voltage waveforms were recorded using LeCroy WaveRunner 6100 A oscilloscope with CP031 hall current sensor and PPE20KV high voltage probe. Figure 3 gives an overview of the experimental setup construction.

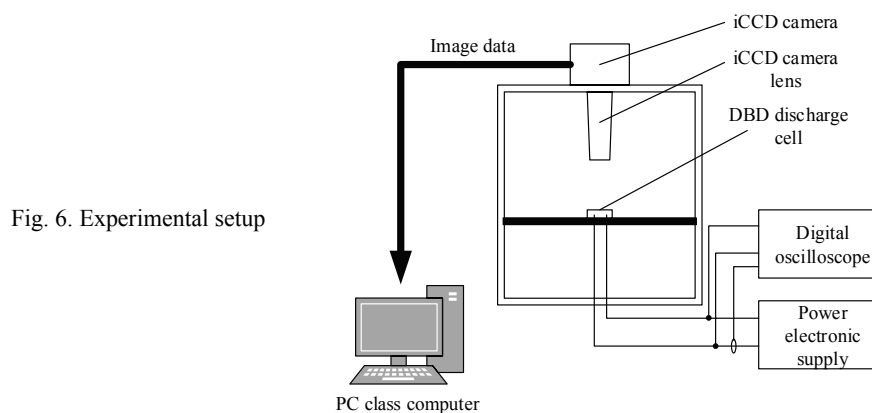


Fig. 6. Experimental setup

Converter produces high voltage peaks with positive pulse duration of 5  $\mu\text{s}$  and rise time of 14.3 V/ns. The oscilloscope waveforms recorded in both discharge cases are depicted in Figure 7. Much less current spikes are observed in the reactor current with saturable inductor implementation, a uniform – like discharge current can be observed in the negative voltage phase with time period of  $6 \div 7 \mu\text{s}$ , as it is presented in Figure 7b. It is assumed that this is due to large time delay between the consecutive pulses. The first half-period of the supply voltage contributes to new charge distribution on the dielectric surface. After discharge ignition, if large volume of the gas gap is conductive, the saturated inductor no longer prohibits intense energy transfer.

The obtained camera and iCCD camera images of the discharge zone are presented in Figure 8 and 9 a, b. The spotted differences show the influence of output inductance on discharge uniformity.

As it can be noticed, a much more intense and homogeneous discharge was observed with the use of saturable inductor. The probable nature of this is the rise time slope of the discharge current and/or the current conduction support by additional inductance during the discharge development. The streamer discharges visible on the outer surface of the dielectric are electrode – dielectric discharges due to the fact that electrodes are not embedded in the dielectric, they are mechanically attached to the outer surface. This effect can be regarded as parasitic discharge. However, the inhibited glow discharge can be assumed, but there is no information available about the exact physics of these discharges [5].

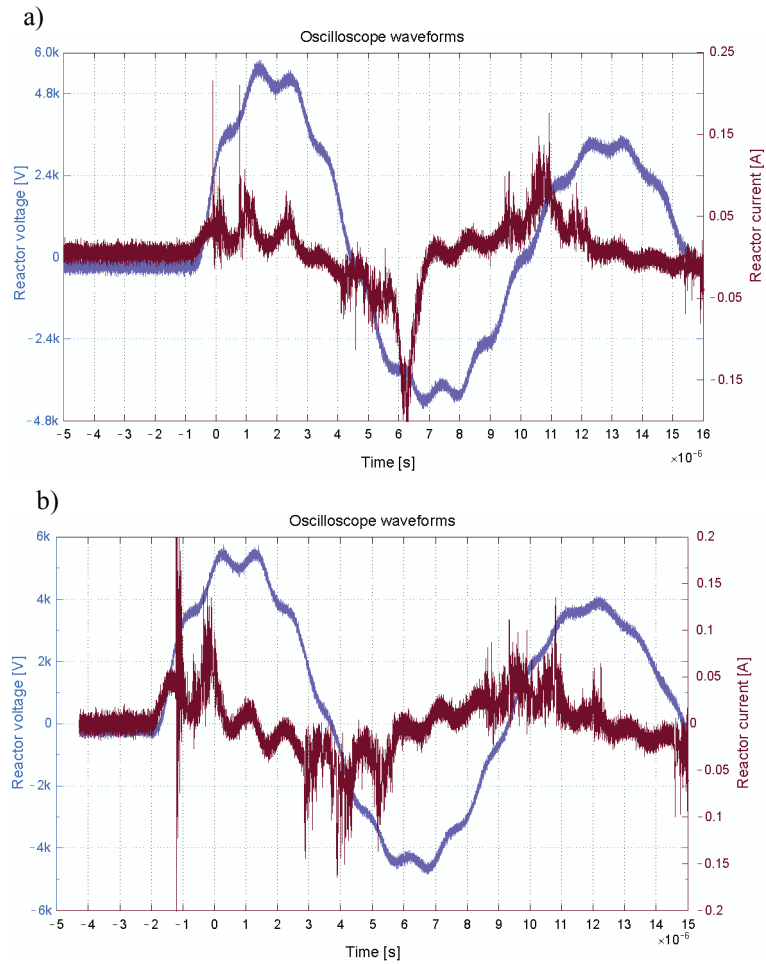


Fig. 7. Recorded oscilloscope waveforms in case of a) no additional inductance, b) saturable inductor

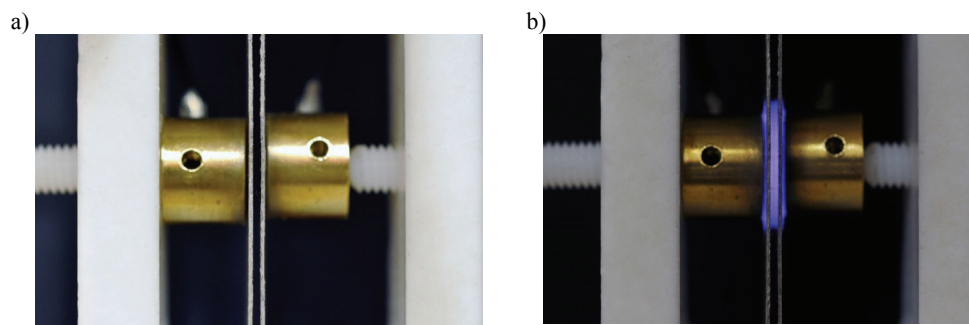


Fig. 8. Camera imaging of the light intensity: a) discharge cell, b) DBD discharge with saturable inductor

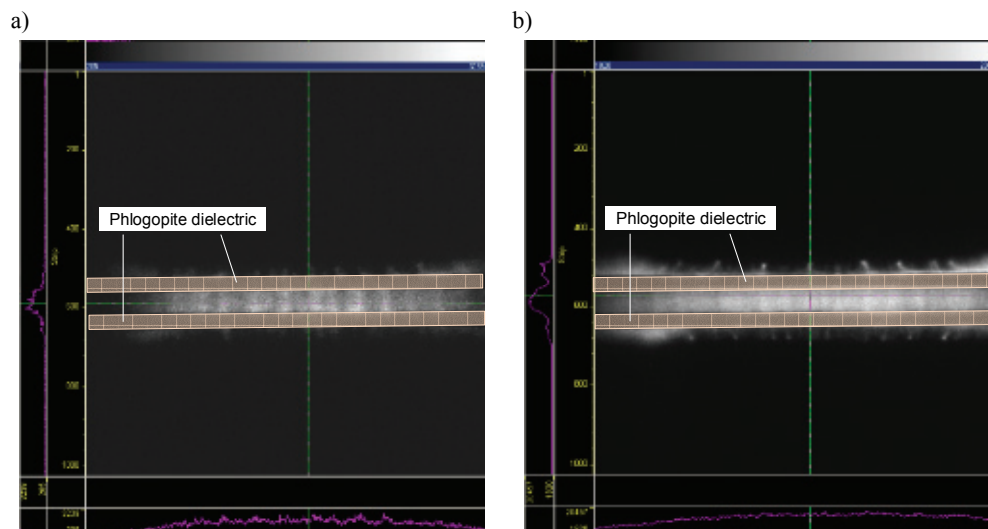


Fig. 9. iCCD camera imaging of the light intensity: a) no additional inductance, b) saturable inductor

## 5. Summary

The presented simulation and experimental study depicts a clear role of the power supply system parameters and voltage waveforms on plasma uniformity. In the presented case quasi-pulsed type supply was investigated, output saturable inductor leads to more uniform plasma distribution and less filamentary character. More attention needs to be given to comparability of the results.

Future studies should involve a more adequate model – based voltage distribution analysis as well as dual mode, transient, finite element method of the electrical field calculations. More detailed analysis and investigations on parameters of the systems with linear, saturable and de-saturable magnetic elements is foreseen.

## References

- [1] Aldea E., Peeters P., De Vries H., Van De Sanden M.C.M., *Atmospheric glow stabilization. Do we need pre-ionization?*, Surface and Coatings Technology 200(1-4): 46-50 (2005), <http://dx.doi.org/10.1016/j.surfcoat.2005.01.052>.
- [2] Massines F., Rabehi A., Philippe D. et al., *Experimental and theoretical study of a glow discharge at atmospheric pressure controlled by dielectric barrier*. Journal of Applied Physics 83(6): 2950, 2957 (1998), doi: 10.1063/1.367051.
- [3] Gherardi N., Massines F., *Mechanisms controlling the transition from glow silent discharge to streamer discharge in nitrogen*. IEEE Transactions on Plasma Science 29(3): 536, 544 (2001), doi: 10.1109/27.928953.
- [4] Radu I., Bartnikas R., Wertheimer M.R., *Frequency and voltage dependence of glow and pseudo-glow discharges in helium under atmospheric pressure*. IEEE Transactions on Plasma Science 31(6): 1363, 1378 (2003), doi: 10.1109/TPS.2003.820970.

- [5] Massines F., Gherardi N., Naudé N., Ségur, *Recent advances in the understanding of homogeneous dielectric barrier discharges*. The European Physical Journal Applied Physics 47 (2009) 22805 doi:10.1051/epjap/2009064.
- [6] Osawa N., Takashi A., Yoshioka Y., Hanaoka R. *Generation of high pressure homogeneous dielectric barrier discharge in air*. The European Physical Journal Applied Physics 61 (2013) 24317 doi:10.1051/epjap/2012120398.
- [7] Sasoh A., Kikuchi K., Sakai T., *Spatio-temporal filament behaviour in a dielectric barrier discharge plasma actuator*. Journal of Physics D: Applied Physics 40(14): 4181 (2007).
- [8] Kostov K., Honda R., Alves L., Kayama M., *Characteristics of dielectric barrier discharge reactor for material treatment*. Brazilian Journal of Physics, São Paulo 39(2) (2009).
- [9] Holub M., Kalisiak S., *Przekształtniki energoelektroniczne dla technologii atmosferycznej plazmy nietermicznej (AP-NTP)*. Polish Electrical Review 86(1): 199-206 (2010).
- [10] Bogaczyk M., Sretenović G., Wagner H.-E., *Influence of the applied voltage shape on the barrier discharge operation modes in helium*. The European Physical Journal D. 67(10): (2013), doi: 10.1140/epjd/e2013-40279-x.
- [11] Francke K.P., Rudolph R., Miessner H., *Design and operating characteristics of a simple and reliable DBD reactor for use with atmospheric air*, Plasma Chemistry and Plasma Processing 23(1), (2003).
- [12] Mok Y., Lee S.-B., Oh J.-H., Ra K.-S., Sung B.-H., *Abatement of Trichloromethane by Using Non-thermal Plasma Reactors*. Journal of Plasma Chemistry and Plasma Processing 28(6) (2008).
- [13] Casanueva R., Azcondo F. J., Bracho S., *Series-parallel resonant converter for an EDM power supply*, Journal of Materials Processing Technology 149: 172-177, (2004).
- [14] Jakubowski T., Kalisiak S., Holub M. et al., *New resonant inverter topology with active energy recovery in PDM mode for DBD plasma reactor supply*. Power Electronics and Applications (EPE 2011), Proceedings of the 2011-14th European Conference on, pp.1, 8 (2011).
- [15] Stryczewska H., Jakubowski T., Kalisiak S. et al., *Power Systems of Plasma Reactors for Non-Thermal Plasma Generation*. Journal of Advanced Oxidation Technologies 16(1): 52-62 (2013).